COMPDYN 2015
5th ECCOMAS Thematic Conference on
Computational Methods in Structural Dynamics and Earthquake Engineering
M. Papadrakakis, V. Papadopoulos, V. Plevris (eds.)
Crete Island, Greece, 25–27 May 2015

MODAL PROPERTIES OF SIMPLY SUPPORTED RAILWAY BRIDGES DUE TO SOIL-STRUCTURE INTERACTION

Christoffer Svedholm[1,2*], Costin Pacoste[1,2] and Raid Karoumi[1]

[1]Division of Structural Engineering and Bridges, KTH Royal Institute of Technology
Brinellvägen 23, 100 44 Stockholm, Sweden

[2] ELU Konsult AB
Valhallavägen 117, 102 51 Stockholm, Sweden
e-mail: christoffer.svedholm@elu.se

Keywords: Bridge, Damping, Soil–structure interaction, Modal properties, Non–proportionally damped

Abstract. *Resonance vibration of railway bridges has become an important design issue during the last decade due to the development of new high-speed lines. At resonance it is well known that the damping of the structure has a great influence on the final response. The current paper presents modal parameters, such as modal damping ratios and natural frequencies, derived based on a simply supported Bernoulli–Euler beam on an elastic half–space.*

In the current chapters of Eurocode dealing with dynamical analysis of railway bridges, the expression for the modal damping ratio is essentially empirical. The novelty of this paper is therefore two-fold: (1) provide modal damping ratios for soil–structure interaction, and (2) show that the damping should not be considered as constant for all modes but it varies depending on the particular mode shape and interaction with the soil.

1 INTRODUCTION

In the field of dynamics, it is well known that damping is of the essence for structures under periodic loading. This would not be a problem in it self but in practice, damping is also the most difficult and complicated problem in vibration. One of the reasons for this seems to be that there exist several mechanisms for energy transfer. Today it is believed that the most important sources of damping for a railway bridge are: (1) bending stresses, (2) friction at supports, (3) wave propagation in soil, and (4) friction in ballast. Given these points, it is not surprising to find that the damping ratios proposed by design handbooks are based on empirical data obtained solely by measuring the free vibration response. The key point is that in this type of measurement the sources of damping are unknown and only the dominant mode is taken into account. For railway bridges, the most well–known and widely used damping ratios (see Fig. 1) are presented in ERRI D-214 [1]. Looking at the figure, it is apparent that there is a pronounced degree of scatter. For example, the ratio of damping for two identical bridges, may vary by a factor 8 [2].

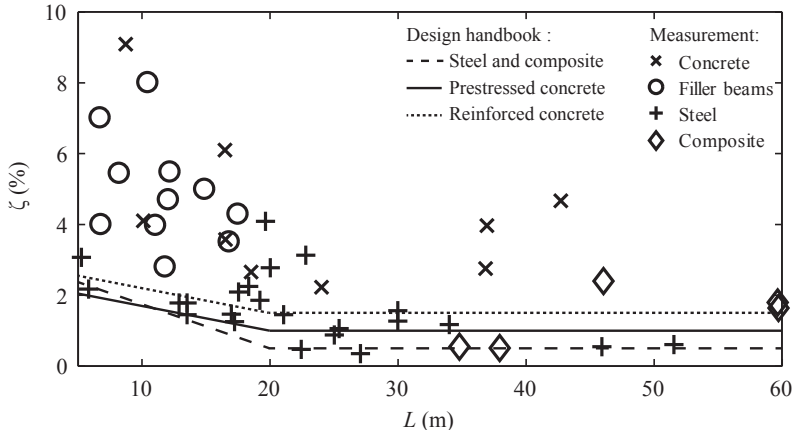

Figure 1: Measured damping values. Reproduced from ERRI D-214 [1]

Therefore, it is the purpose of this paper to provide new insight to this problem. Here, we focus on soil-structure interaction (SSI). Ülker et al. [8] performed the dynamic analysis of a portal frame bridge to study the effect of soil–structure interaction. Through numerical simulation, it was found that the modal damping ratio could vary between 1 and 15%. In another interesting paper, Romero et al. [7] studied soil–structure interaction in resonant railway bridges. It is shown by means of numerical calculations that soft soils have a favourable effect on the response due to geometric damping.

The novelty of this paper is to perform a thorough investigation of modal parameters due to SSI in railway bridges. For this purpose, we begin by deriving an analytical expression for the natural frequencies and modal damping ratios of an elastically–supported beam with two vertical viscous dampers. An approximation of the spring–dashpot parameters can be found from Gazetas model [4]. Based on this model, we are able to address several important questions. In particular, good correspondence is found between theoretical and measured damping values.

2 FORMULATION OF THE PROBLEM

Let us start by considering Fig. 2, a Bernoulli–Euler beam supported by a spring–dashpot system representing the elastic half–space. Then, the equation of motion for free vibration is given by,

$$m\frac{\partial^2 w}{\partial t^2} + EI\frac{\partial^4 w}{\partial x^4} = 0 \tag{1}$$

where the mass per unit length m and bending stiffness EI are assumed constant over the span L.

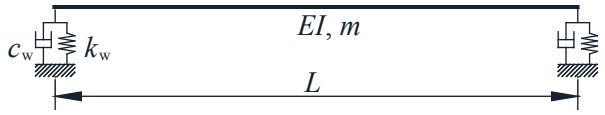

Figure 2: Structural system of an elastically–supported beam with two vertical viscous dampers.

Using the separation–of–variables technique, the transverse displacement $w(x,t)$ can be written as a product of two functions, each depending only on one parameter:

$$w(x,t) = q(t)\phi(x) \tag{2}$$

Here $q(t)$ is the generalized coordinate and $\phi(x)$ is the normal mode. Then, by substituting Eq. 2 into Eq. 1 and grouping all terms involving t and x on the left–hand side and right–hand side, respectively, we obtain Eq. 3.

$$\frac{\ddot{q}(t)}{\frac{EI}{m}q(t)} = -\frac{\phi''''(x)}{\phi(x)} \tag{3}$$

Now Eq. 3 can be reduced to a pair of ordinary differential equations by making each side of the equation equal a constant $-\lambda^4$.

$$\phi''''(x) - \lambda^4\phi(x) = 0 \tag{4a}$$

$$\ddot{q}(t) + \lambda^4\frac{EI}{m}q(t) = 0 \tag{4b}$$

The solution to the above equations are of the form:

$$\phi(x) = A_1e^{\lambda x} + A_2e^{-\lambda x} + A_3e^{i\lambda x} + A_4e^{-i\lambda x} \tag{5a}$$

$$q(t) = Be^{\Lambda t} \tag{5b}$$

A relationship between the separation constant λ and the eigenvalue Λ is obtained by substituting Eq. 5b into Eq. 4b.

$$\lambda^4 = -\frac{m\Lambda^2}{EI} \tag{6}$$

We have now to introduce the boundary conditions to be able to calculate Λ and $A_1 - A_4$. From the free body diagram (Fig. 3) it follows that the sum of forces and moments, at $x = 0$ and

$x = L$, should be zero:

$$EI\phi'''(0) = -Z_w(\Lambda)\phi(0) \tag{7a}$$
$$EI\phi''(0) = 0 \tag{7b}$$
$$EI\phi'''(L) = Z_w(\Lambda)\phi(L) \tag{7c}$$
$$EI\phi''(L) = 0 \tag{7d}$$

where the impedance is evaluated as $Z_w(\Lambda) = c_w\Lambda + k_w$. Now, by substituting Eq. 5a into

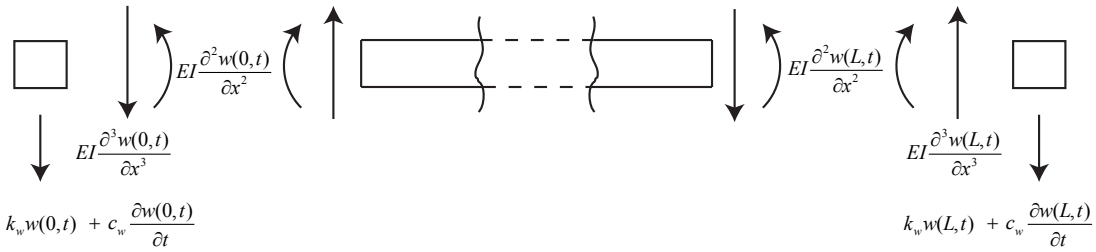

Figure 3: Free body diagram.

Eq. 7 and arranging the four equations into matrix form, i.e. $\Gamma(\Lambda)J = 0$, we obtain:

$$\begin{bmatrix} \eta+1 & \eta-1 & \eta-i & \eta+i \\ -(\eta-1)\,e^{L\lambda} & -(\eta+1)\,e^{-L\lambda} & -(\eta+i)\,e^{L\lambda i} & -(\eta-i)\,e^{-L\lambda i} \\ 1 & 1 & -1 & -1 \\ e^{L\lambda} & e^{-L\lambda} & -e^{L\lambda i} & -e^{-L\lambda i} \end{bmatrix} \begin{bmatrix} A_1 \\ A_2 \\ A_3 \\ A_4 \end{bmatrix} = \begin{bmatrix} 0 \\ 0 \\ 0 \\ 0 \end{bmatrix} \tag{8}$$

where $\eta = Z_w/\lambda^3 EI$. The eigenvalues are calculated by solving $\mathrm{Det}(\Gamma) = 0$. Once the eigenvalues have been estimated, it is possible to calculate the angular natural frequency ω_n and the modal damping ration ζ_n.

$$\omega_n = |\Lambda_n| \tag{9a}$$
$$\zeta_n = \frac{-\Re(\Lambda_n)}{\omega_n} \tag{9b}$$

The angular natural frequency of vibration is given by the familiar equation $\omega_n = 2\pi f_n$, where f_n is the natural frequency of vibration.

3 SOIL–STRUCTURE INTERACTION

Through the years, there have been a number of studies looking at soil–structure interaction (SSI) during dynamic loading. In the authors' opinion, the most comprehensive work in this area is due to Gazetas [4, 3, 5]. The present paper uses Gazetas solution for a rigid slab on an elastic half–space to calculate spring and dashpot coefficients. Hereafter, for the sake of completeness, we provide a brief summary of Gazetas method [4].

First, let us consider a general shape foundation with a soil contact area of A_b and a circumscribed rectangle $2B_1$ by $2B_2$, where $B_1 \geq B_2$. Once the geometry of the slab and the soil properties are known, the dynamic stiffness k_w can be calculated with the following equation:

$$k_w = \frac{2GL}{1-\nu}\left(0.73 + 1.54\chi^{0.75}\right)\tilde{k}_w\left(B_1/B_2, \nu; a_0\right) \tag{10}$$
$$\text{where } \chi = \frac{A_b}{4L^2}$$

Here the dynamic stiffness coefficient $\tilde{k}_w$ (Fig. 4) accounts for the frequency–dependent effects. It is important to note that frequency–dependent parameters only arise if the half space is replaced by a spring-dashpot model. In Fig. 4, the dimensionless circular frequency is defined by $a_0 = \omega B_2/V_\mathrm{s}$, where V_s stands for the shear wave speed. The radiation dashpot, c_w, which accounts for the spreading of elastic waves in the half–space medium, is defined by:

$$c_w = \rho V_\mathrm{La} A_\mathrm{b} \tilde{c}_w\left(B_1/B_2, \nu; a_0\right) \tag{11}$$
$$\text{where } V_\mathrm{La} = \frac{3.4V_\mathrm{s}}{\pi\left(1-\nu\right)}$$

The radiation dashpot coefficient $\tilde{c}_w$ is plotted in Fig. 4. It should also be noted here that $\tilde{c}_w$ varies with frequency. However, from the figure it is evident that frequency dependence is relatively small for $B_1/B_2 < 6$. The variable V_La in Eq. 11 is known as Lysmer's analog wave velocity, which physically represents the velocity of compression waves at the foundation–soil interface.

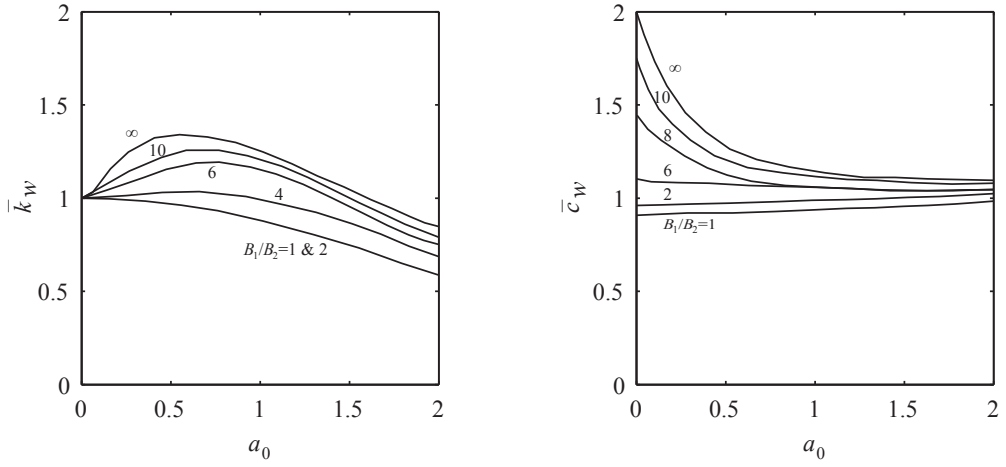

Figure 4: Dynamic stiffness and dashpot coefficient. Reproduction from Gazeta [4]

4 NUMERICAL EXAMPLES

Numerical simulations have been performed on bridges with a span of 5 m (short) to 60 m (long) supported by a granular material with a Young's modulus E_{soil} of 50 MPa (loose) to 800 MPa (dense). The Poisson's ratio and density of the soil was assumed constant $\nu = 0.4$ and $\rho = 1800$ kg/m^3, respectively. Also, the size of the foundation is fixed to a constant value of 8×8 m. Both the mass per unit length m and the bending stiffness EI was assumed to vary with the span L. This relationship was previously derived in Johansson et al. [6], where Eq. 12a and 12b are proposed, for single–track ballasted concrete bridges, by collecting data from "real" bridges.

$$m = 580L + 5350 \text{ [kg/m]} \tag{12a}$$

$$EI = 4(265L^{-1.28})^2 mL^4/\pi^2 \text{ [N/m}^2\text{]} \tag{12b}$$

On the basis of this information, numerical simulation have been carried out in MATLAB R2013a to determine natural frequencies, modal damping ratios and mode shapes.

4.1 Loose granular material

This section presents the results, see Fig. 5 and Table. 2, for a loose soil with an elastic Young's modulus of 50 MPa. Using the parameters presented above, this corresponds to a shear wave speed of $V_s = 99.6$ m/s. By examining the figures, it turns out that the solution consist of a set of underdamped (bending mode 1-6) and overdamped (mode 7-10) modes, hereafter, these modes are referred to as "real" and "imaginary" modes, respectively. If we only consider

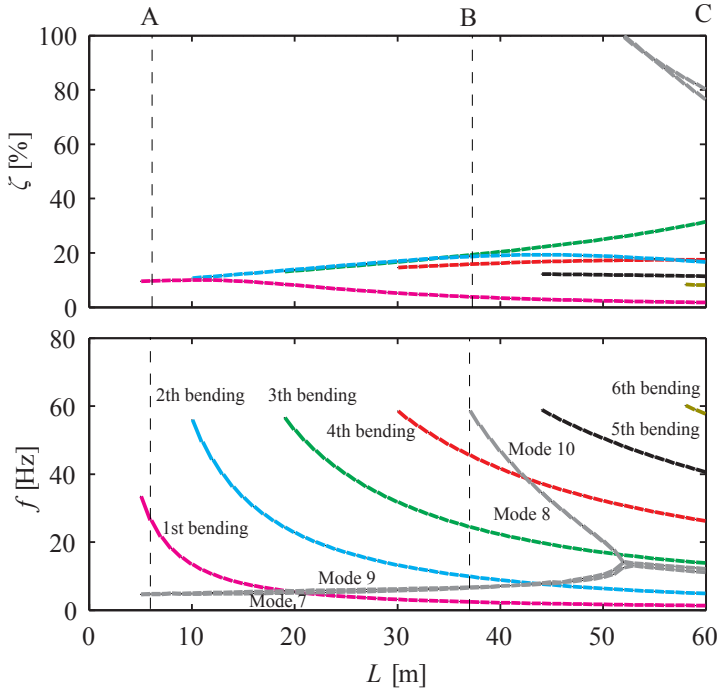

Figure 5: Damping ratios and natural frequencies for $E_{\text{soil}} = 50$ MPa.

the imaginary modes, it seems that something interesting is happening at $L = 52$ m. This is because at $L < 52$ m there exist four imaginary modes with $\zeta > 1$, but at $L > 52$ m these merge into two modes with $\zeta < 1$. The reason for this is not clear, but it could be that the wave

propagation characteristics change. Let us then consider the modal damping ratios of the real modes in Fig. 5. Here the results show that the modal damping ratio varies depending on the particular mode shape and span. The smallest (1.75 %) and largest (31.4 %) damping ratios were, for example, obtained at $L = 60$ m, for the 1st and 3rd bending mode, respectively. This difference is most easily explained by looking at the modal displacement and phase angle of the relevant modes (see Table. 2 Case C). Here it is obvious that the 1st bending mode is dominated by standing wave (all points in–phase or out–of–phase) and the 3th bending mode is vibrating in a combination of traveling and standing wave. Finally, Table. 1 show the maximum damping ratio for the bending modes.

Table 1: Maximum damping ratios for $E_{\text{soil}} = 50$ MPa.

	1st bending	2th bending	3th bending	4th bending	5th bending	6th bending
L [m]	11	42	60	60	44	58
ζ_n [%]	10.0	19.3	31.4	17.5	12.2	8.3

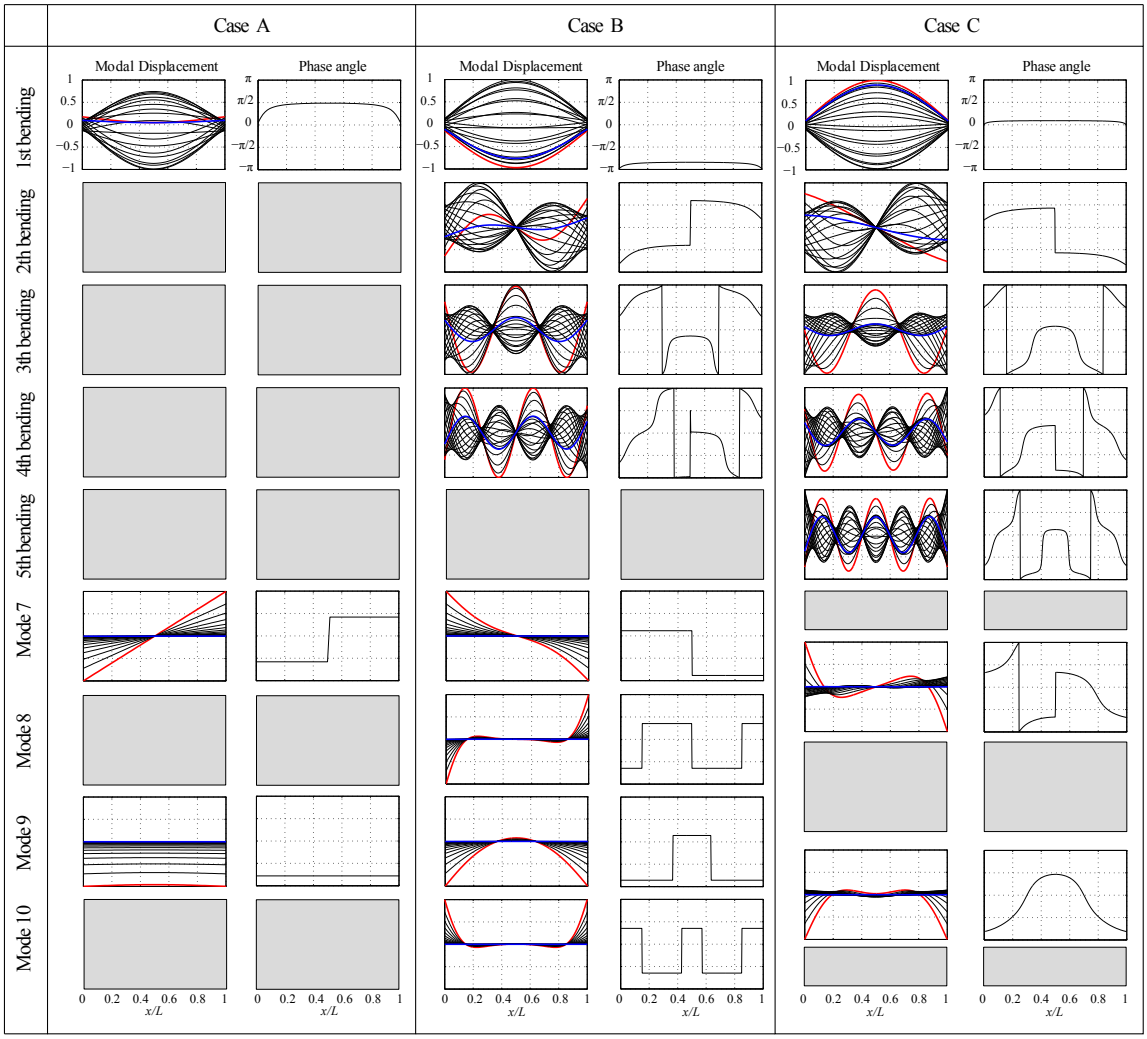

Table 2: Modal displacement and phase angle for $E_{\text{soil}} = 50$ MPa.

4.2 Dense granular material

The results presented in Section 4.1 show that loose soils provide high modal damping values. However, these values are drastically reduced for dense soils. Taking for illustrative purposes $E = 200$ MPa ($V_s = 199.2$ m/s, see Fig. 6 and Table 4), we find that ζ, at $L = 60$ m, varies from 0.3 % (1st bending) to 12.9 % (4th bending). This corresponds to a reduction of the modal damping ratio by 82.9 % and 58.9 %. With this in mind the engineer should, when designing a bridge, use stiff material for the soil in order not to overestimate the damping.

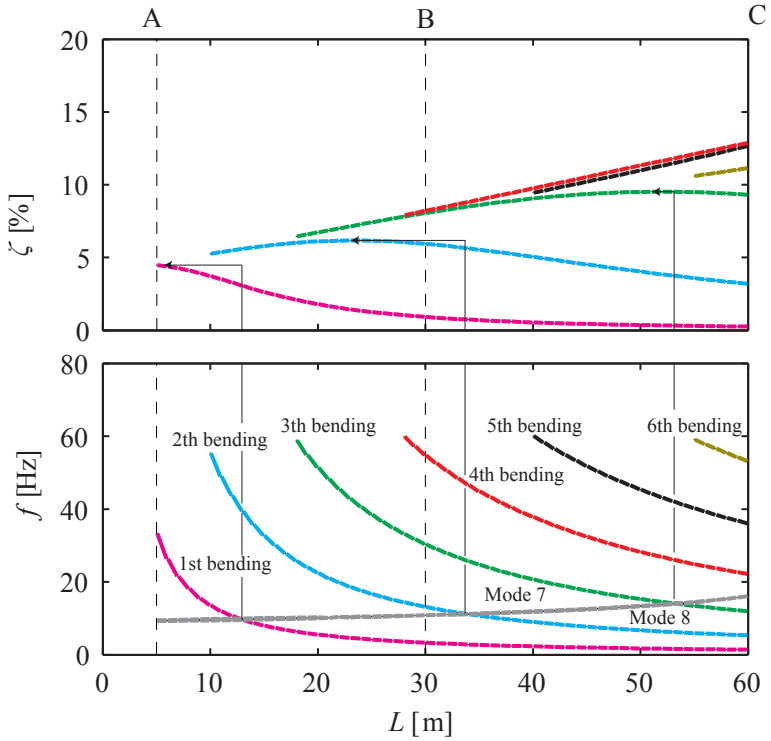

Figure 6: Damping ratios and natural frequencies for $E_{\text{soil}} = 200$ MPa.

For both soil types, it was found that ζ_n tends to $\uparrow$ (increase) with the first few modes, after which ζ_n tends to $\downarrow$ (decreases), see Table. 1 and 3. In fact, if we let $n \to \infty$, then the model shows that $\zeta_n \to 0$. To put the same thing in other words, SSI cannot damp the high frequency oscillation in general. Another aspect that the authors found interesting is that maximum damping seem to occur in the vicinity points where the natural frequencies of real and imaginary modes coincide. This observation, together with previous studies by the authors show that imaginary modes provide damping to real modes if their natural frequencies are closely spaced.

Table 3: Maximum damping ratios for $E_{\text{soil}} = 200$ MPa.

	1st bending	2th bending	3th bending	4th bending	5th bending	6th bending
L [m]	5	23	51	60	60	60
ζ_n [%]	4.5	6.2	9.5	12.9	12.7	11.1

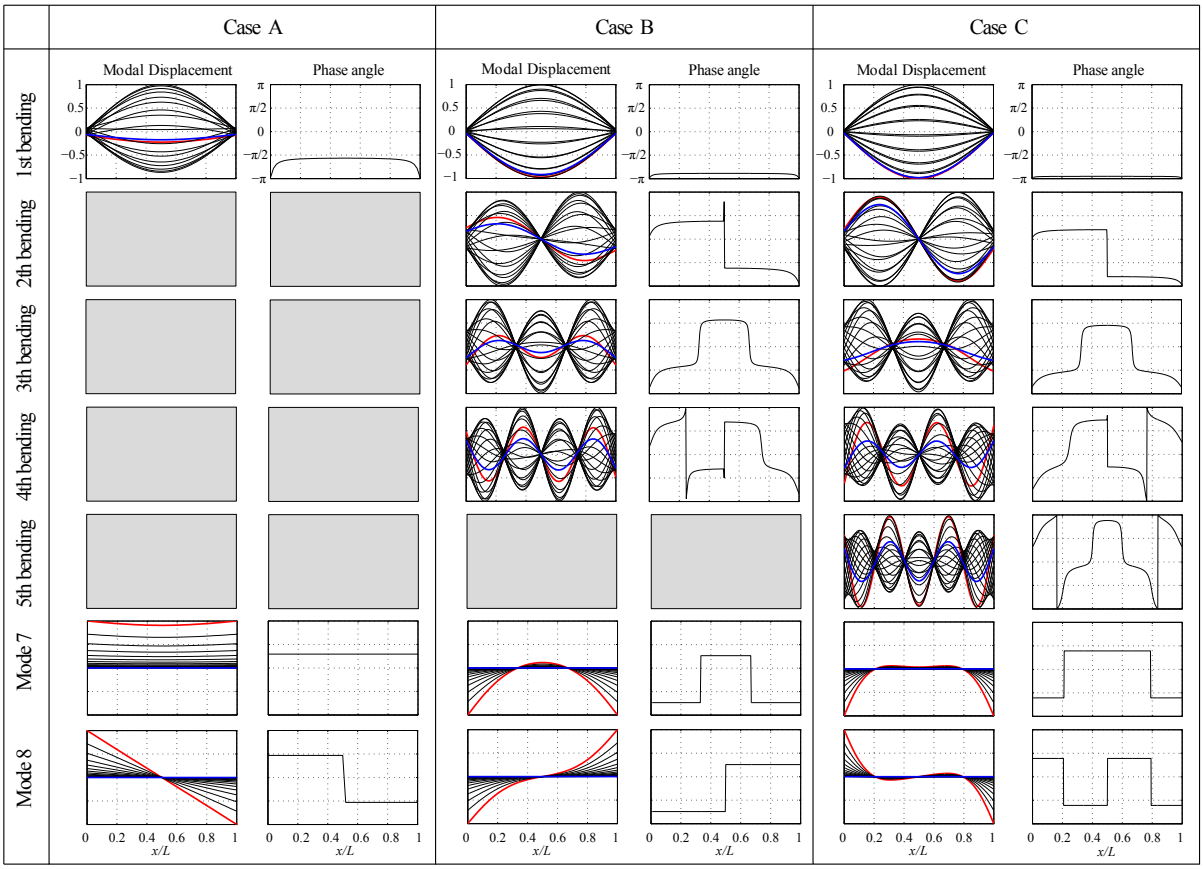

Table 4: Modal displacement and phase angle for $E_{\text{soil}} = 200$ MPa.

4.3 Damping of the fundamental frequency

In this section, we compare measured and calculated modal damping ratios for the 1st bending mode. Higher modes of vibration are not studied due to limited amount of published experimental data. The measured data points, in Fig. 7, are reproduced from a plot in reference [1]. A fairly reasonable interpretation of the scattering in the figure might be that the modal damping ratio cannot be uniquely defined by the span and type of bridge. Here, we propose that the foundation is another important aspect, which needs to be studied in detail to accurately predict the damping of each mode. To exemplify this fact, we also present in Fig. 7 numerically calculated modal damping ratios (solid lines) of the 1st bending mode for soils with $E_{\text{soil}} = 50 - 800$ MPa. Looking at the figure one can see good consistency between experimental and numerical data. Namely, the modal damping ratio is of the right magnitude and tends to decrease with the span. From a practical point of view, a typical soil in Sweden lies between 100 MPa and 400 MPa. Damping ratios for soils outside of this range should therefore be considered as a theoretical exercise. With this in mind, the expected damping ratio from soil alone is between 0.1 % (long span & dense soil) and 6.6 % (short span & loose soil). This findings clearly indicate that geometric damping of soil is one of the main contributor to damping in railway bridges.

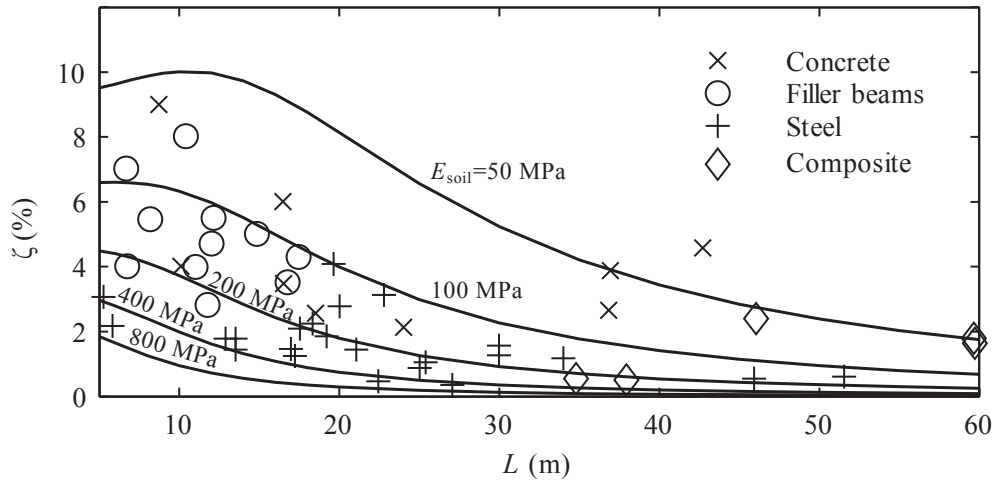

Figure 7: Damping of the 1st bending mode as a function of span. The solid lines are the simulated results.

5 CONCLUSIONS

In this paper, a model for calculating modal properties of a Bernoulli–Euler beam, supported by an elastic half–space, is derived. The model is then used to study the effects of soil–structure interaction (SSI) for ballasted reinforced concrete bridges. From these numerical results, it is possible to draw the following conclusions:

- The expected damping ratio for the 1st bending mode from soil alone is between 0.1 % and 6.6 % for a long span bridge supported by a dense soil and a short span bridge supported by a loose soil, respectively.
- The results of the calculation show that traveling waves provide a damping ratio of 6-12.9 % to the 2-6th bending mode for medium to long span bridges.
- A good correlation is found between theoretical and measured damping values for the 1st bending mode. Higher modes of vibration are not studied due to limited amount of published experimental data.
- SSI will only damp the first few bending modes.
- It is found that imaginary modes provide damping to real modes if their natural frequencies are closely spaced.

REFERENCES

[1] ERRI D-214. Rail bridges for speeds over 200km/h, final report, 1999.

[2] ERRI D-214. Rail bridges for speeds over 200km/h, recommandations for calculating damping in rail bridge decks, 1999.

[3] G Gazetas. Analysis of machine foundation vibrations: state of the art. *International Journal of Soil Dynamics and Earthquake Engineering*, 2(1):2–42, 1983.

[4] G Gazetas. Foundation engineering handbook, chapter 15, 1991.

[5] G Gazetas, K Fan, and A Kaynia. Dynamic response of pile groups with different configurations. *Soil Dynamics and Earthquake Engineering*, 12(4):239–257, 1993.

[6] C. Johansson, A. Andersson, J. Wiberg, M. Ülker-Kaustell, C. Pacoste, and R. Karoumi. Höghastighetsprojekt-bro: Delrapport i: Befintliga krav och erfarenheter samt parameterstudier avseende dimensionering av järnvägsbroar för farter över 200 km/h. 2010.

[7] A. Romero, M. Solís, and P. Galvín. Soil-structure interaction in resonant railway bridges. *Soil Dynamics and Earthquake Engineering*, 2012.

[8] M Ülker-Kaustell, R Karoumi, and C Pacoste. Simplified analysis of the dynamic soil–structure interaction of a portal frame railway bridge. *Engineering structures*, 32(11):3692–3698, 2010.